

Canopy photosynthesis modulates soil respiration in a temperate semi-arid shrubland at multiple timescales

Xin Jia · Tianshan Zha · Shan Wang · Charles P.-A. Bourque · Ben Wang · Shugao Qin · Yuqing Zhang

Received: 20 April 2018 / Accepted: 13 September 2018 / Published online: 20 September 2018
© Springer Nature Switzerland AG 2018

Abstract

Aims Soil respiration (R_s) plays an important role in the terrestrial carbon cycle, but how canopy photosynthesis and abiotic drivers interact to affect R_s is poorly understood. This study aimed at examining the degree of control gross ecosystem productivity (GEP), photosynthetically active radiation (PAR), and soil temperature (T_s) and water content (SWC) may have on R_s in a semi-arid shrub ecosystem.

Methods We applied wavelet analysis and non-parametric spectral Granger-causality to a multi-year dataset.

Results Wavelet coherence revealed synchronized diel cycles in photosynthesis proxies (GEP and PAR) and R_s . The spectral Granger-causality analysis suggested a possible

causal linkage between GEP and R_s at the diel scale during the growing season. Significant wavelet coherence was also observed between GEP and R_s at seasonal to annual scales (200–365-day periods), with R_s lagging GEP by an average of two days. Fluctuations in SWC showed non-continuous temporal covariance with R_s over 4–64-day periods. Apart from direct moisture effects on decomposition processes, SWC also seemed to regulate R_s indirectly by affecting canopy carbon assimilation.

Conclusion Our findings indicate that photosynthesis may modulate R_s at multiple timescales in semi-arid shrub ecosystems. Future studies should combine field manipulations with spectral analysis for a mechanistic understanding of the coupling between photosynthesis and R_s .

Responsible Editor: Lucas Silva.

Electronic supplementary material The online version of this article (<https://doi.org/10.1007/s11104-018-3818-z>) contains supplementary material, which is available to authorized users.

X. Jia · T. Zha (✉) · S. Wang · C. P.-A. Bourque ·
B. Wang · S. Qin · Y. Zhang

Yanchi Research Station, School of Soil and Water Conservation,
Beijing Forestry University, PO Box 67, #35 East Qinghua Rd.,
Haidian District, Beijing 100083, China
e-mail: tianshanzha@bjfu.edu.cn

X. Jia · T. Zha · S. Wang · B. Wang · S. Qin · Y. Zhang
Key Laboratory for Soil and Water Conservation, State Forestry
Administration, Beijing Forestry University, Beijing 100083,
China

C. P.-A. Bourque
Faculty of Forestry and Environmental Management, University
of New Brunswick, Fredericton, NB E3B 5A3, Canada

Keywords Gross ecosystem production · Lag · Shrub ·
Soil CO₂ efflux · Substrate · Wavelet analysis

Introduction

Soil respiration (R_s) is the second largest terrestrial CO₂ flux following gross ecosystem productivity (GEP), and contributes to 50–80% of total ecosystem respiration (Bond-Lamberty and Thomson 2010; Janssens et al. 2001). Slight changes in R_s may alter ecosystem carbon (C) budgets, which may in turn influence regional and global climate by various feedback processes (Luo 2007). Therefore, understanding the biophysical controls on R_s is essential for predicting ecosystem C balance under climate change. Soil respiration is affected by a number of abiotic (e.g. soil temperature and moisture) and biotic

factors (e.g. plant functional type, root density, microbial community composition, photosynthetic activity, and fresh litter availability; Barron-Gafford et al. 2011; Luo and Zhou 2006). Substantial progress has been made in understanding the relationships between R_s and biophysical variables at diel, seasonal, and interannual timescales (Barron-Gafford et al. 2011; Wang et al. 2017). However, considerable uncertainty still exists regarding the response of R_s to biophysical variables across these timescales.

The relative importance of temperature and plant photosynthesis in controlling R_s has been a topic of sustained interest in recent years (Heinemeyer et al. 2012; Kuzyakov and Gavrichkova 2010; Tang et al. 2005; Vargas et al. 2011). Diurnal and seasonal variations in R_s have traditionally been represented as empirical functions of soil temperature (T_s) or as functions of T_s and soil water content (SWC) for different ecosystems (Carbone et al. 2008; Jia et al. 2013; Wang et al. 2014). However, field data suggest that T_s and SWC alone may not adequately represent R_s over multiple timescales. Eco-physiological factors, such as photosynthesis, phenology, and fine root turnover may be as important to the representation and prediction of R_s (Han et al. 2014; Reichstein et al. 2003; Vargas et al. 2011). Organic matter produced by plant photosynthesis is the ultimate source of C for all R_s components. Autotrophic respiration is fueled by current or recent photosynthates and stored carbohydrates (Bahn et al. 2009; Carbone et al. 2008). Rhizospheric microbial activity can be stimulated by root exudates (Högberg et al. 2009; Savage et al. 2013). Free-living microbes serve to rapidly decompose fresh leaf and root litter (Gaumont-Guay et al. 2008). From this, it is reasonable that R_s may be better represented by photosynthesis than by T_s .

Earlier studies have provided evidence that R_s is strongly associated with canopy photosynthesis at different timescales. Increasing evidence suggests that current or recent photosynthates modulate diel variations in R_s (Bahn et al. 2009; Han et al. 2014; Tang et al. 2005). Several studies in forests and grasslands showed that R_s may be largely fueled by plant carbohydrate storage with different turnover rates, leading to a coupling between photosynthesis and R_s at timescales of days to weeks (Carbone and Trumbore 2007; Carbone et al. 2008; Heinemeyer et al. 2012; Mencuccini and Hölttä 2010). In addition, dependence of R_s on ecosystem productivity was observed to occur for different ecosystems at seasonal and annual timescales (Bahn et al. 2008; Janssens et al. 2001; Sampson et al. 2007; Vargas et al. 2010a). The importance of photosynthesis in regulating R_s can be anticipated in

drylands (i.e. semi-arid and arid areas), where rhizospheric respiration is more likely to dominate R_s , due to normally low soil organic carbon (SOC) content and microbial biomass in these areas. However, limited information is available on the multi-temporal relationship between photosynthesis and R_s in semi-arid shrub ecosystems, which constitute an important land-cover type in Eurasia.

Although photosynthesis is considered an important process affecting R_s , articulating their coupling is often limited by measurement and analytical techniques, and complicated by confounding abiotic factors (e.g. T_s , SWC, and soil CO₂ transport) (Detto et al. 2012; Vargas et al. 2011). Accumulating long-term, hourly R_s data measured with auto-chambers provide an opportunity to investigate in detail the timing, time lags, and effective timescales regarding biophysical controls on R_s (Vargas et al. 2010a, b). Application of spectral analyses to these measurements could help resolve the mechanisms regulating terrestrial CO₂ fluxes across multiple timescales (Detto et al. 2012; Vargas et al. 2010b, 2011). For example, wavelet coherence (WTC) analysis has been used to investigate the level of coupling between biophysical factors and ecosystem CO₂ and water fluxes across the time-frequency domain in forests, grasslands, and croplands (e.g. Barba et al. 2018; Vargas et al. 2010b, 2011, 2012). Non-parametric spectral Granger-causality enables a stronger indication of scale-specific causality between processes than does WTC, although the former does not provide detailed information on when the coupling occurs (Detto et al. 2012). We are not aware of any other study using such complementary spectral analyses to explore ecological processes in semi-arid shrub ecosystems.

In this study, we applied spectral analysis on a multi-year dataset (June 2012–November 2015, see the on-line supplementary material) to examine the degree of control GEP, photosynthetically active radiation (PAR), T_s , and SWC may have on R_s in a semi-arid shrub ecosystem. We hypothesized that canopy photosynthesis is the main driver of R_s dynamics at diel and seasonal to annual timescales. We also suspected that canopy photosynthesis affects R_s at intermediate scales of days, weeks, to months.

Materials and methods

Study site

The study site was located at the Yanchi Research Station (37°42'31"N, 107°13' 37"E; 1530 m a.s.l.),

Ningxia, northern China. The site is representative of a transition zone between arid and semi-arid climate at the southern edge of the Mu Us Desert, with *Artemisia ordosica* and *Hedysarum mongolicum* being the dominant shrub species. Other shrub and grass species include *Hedysarum scoparium*, *Salix psammophila*, *Leymus secalinus*, *Pennisetum centrasiticum*, and *Stipa glareosa*. The shrub canopy was about 0.5–1.0 m tall. The mean annual temperature (1954–2014) at the site is 8.3 °C, and the mean monthly temperature ranges from –8.4 °C in January to 22.7 °C in July (data from Yanchi Meteorological Station, about 20 km from the study site). The mean annual precipitation is 292 mm, nearly an order of magnitude lower than mean annual potential evapotranspiration (2024 mm). In addition, precipitation at the site is characterized by large seasonal (about 80% falling during June–September) and interannual variability (145–587 mm, from 1954 to 2014). Soil water availability depends entirely on precipitation, due to a deep groundwater table (> 8 m). The soil is an aripsamment (USDA soil taxonomy) with more than 70% of its dry weight consisting of fine sand (0.02–0.20 mm grain size). The soil has a bulk density of $1.54 \pm 0.08 \text{ g cm}^{-3}$ (mean \pm standard deviation, $n = 16$) in the upper 10 cm of the soil profile (Jia et al. 2014). The total soil porosity within 0–2 and 5–25 cm depths was 50 and 38%, respectively (Wang et al. 2017). Soil organic C, total nitrogen and pH in the surface layer (0–5 cm) were 3.4–21.4 g kg⁻¹, 0.20–1.0 g kg⁻¹, and 7.8–8.8, respectively (Feng et al. 2014).

Field measurements

This study used hourly soil CO₂ efflux measurements from 3 June 2012–12 November 2015. This period was preceded and followed by large data gaps that may have caused uncertainties in gap-filling and biases in analyses. Soil CO₂ efflux was measured using an automated chamber system (LI-8100A equipped with a LI-8150 multiplexer, LI-COR, USA) with 11 chambers (LI-104, LI-COR, USA). These chambers were randomly deployed within a 15 m radius from the multiplexer to account for the spatial variability in R_s . As our research questions address the periodicity of R_s and linkages to canopy photosynthesis over multiple time-scales, rather than the spatial pattern in R_s , we averaged soil CO₂ effluxes over all chambers to represent R_s in the ecosystem of interest. Each chamber was attached to a PVC collar (20.3 cm in inner diameter, 10 cm in height) that was inserted into the soil to a depth of 7 cm. All collars

were installed 3 months before the first CO₂ efflux measurements. All plants inside the collars were clipped to the ground surface when installing the collars and any regrowth was clipped on a regular basis. Hourly T_s and SWC were measured at a 10-cm depth adjacent to each collar with 8150–203 soil temperature (LI-COR, USA) and ECH₂O Model EC-5 soil moisture probes (Decagon Devices, USA), respectively. Soil CO₂ efflux measurements are described in more detail by Wang et al. (2014).

Estimates of GEP were derived from half-hourly eddy-covariance (EC) measurements of net ecosystem CO₂ exchange (NEE). The EC system consists of a 3D ultrasonic anemometer (CSAT-3, Campbell Scientific, USA) and a closed-path infrared gas analyzer (LI-7200, LI-COR, USA), both mounted on a scaffold tower at a 6.2-m height above the ground. The flux tower was about 500 m from the soil chamber system. Uncertainties and biases could have possibly arisen in our comparison of GEP and R_s , since 90% of the flux-measurement footprint (within 200 m of the tower; Jia et al. 2014) was peripheral to the measurement footprint of the soil chamber system. However, the underlying surface was generally homogeneous within 1 km of the tower in terms of topography, vegetation, and edaphic conditions (Jia et al. 2016; Wang et al. 2014). Given the study's focus on variations and periodicities in these fluxes, possible biases between fluxes became less important. We argue that the footprint mismatch between GEP and chamber-based R_s measurements had marginal effect on our main conclusions.

Incident PAR was measured with a quantum sensor (PAR-LITE, Kipp & Zonen, The Netherlands) mounted at 6.0 m height on the flux tower. Rainfall was measured daily with a manual rain gauge before 22 July 2012 and with a tipping-bucket rain gauge thereafter (TR-525 M, Texas Electronics, USA) at a distance of about 50 m from the tower. The reader is referred to Jia et al. (2014, 2016) for a detailed description of EC instrumentation, data quality control, gap-filling, and flux partitioning.

Data processing and analysis

Soil respiration measurements outside the range of -1 – $15 \mu\text{mol CO}_2 \text{ m}^{-2} \text{ s}^{-1}$ were considered abnormal and hence rejected (Wang et al. 2014, 2015). Soil respiration values smaller than $-1 \mu\text{mol CO}_2 \text{ m}^{-2} \text{ s}^{-1}$ were caused by instrument malfunctions, and those larger than $15 \mu\text{mol CO}_2 \text{ m}^{-2} \text{ s}^{-1}$ occurred when ants colonized the soil within the collar.

Slightly negative values ($-1-0 \mu\text{mol CO}_2 \text{ m}^{-2} \text{ s}^{-1}$, accounting for 2.5% of all values) were valid measurements during cold winters or precipitation events. Instrument failure and quality control together resulted in 10% missing values over the study period (3 June 2012–12 November 2015). Gaps in the hourly R_s timeseries were filled using the mean diurnal variation method (Falge et al. 2001).

Here, we briefly describe the core concepts of continuous wavelet transform (CWT), cross-wavelet transform (XWT), WTC, and partial wavelet coherence (PWC). Detailed review of the theory and application of wavelet analysis can be found in Torrence and Compo (1998), Grinsted et al. (2004), Cazelles et al. (2008), and Ng and Chan (2012).

We used CWT to identify the periods (i.e. time-scales) at which variability in a timeseries (i.e. R_s or biophysical factors) occurs. Continuous wavelet transform of a discrete signal x_n of length (N) recorded at interval δt is defined as the convolution integral:

$$W_n^x(s) = \sqrt{\frac{\delta t}{s}} \sum_{n'=1}^N x_{n'} \psi_0^* \left[\frac{(n'-n)\delta t}{s} \right], \quad (1)$$

where ψ_0^* is the complex conjugate of the scaled and translated mother wavelet, and s is the wavelet scale at which the transform is applied (Grinsted et al. 2004). We used the Morlet wavelet as the mother wavelet because it provides a good balance between the localization of time and frequency (Vargas et al. 2010b), and it is able to produce a smooth depiction of non-stationary processes in the time-frequency domain (Heinemeyer et al. 2012). Moreover, the Morlet wavelet is a complex function (i.e. with both a real and an imaginary part), thus allowing for separate investigations of phases and amplitudes (Grinsted et al. 2004).

The wavelet power spectrum (S_n) of x_n is defined as:

$$S_n(s) = |W_n^x(s)|^2. \quad (2)$$

Peaks in the global wavelet spectrum (i.e. S_n averaged over time) provide information on the periods contributing the most to the variability of a timeseries (Vargas et al. 2010b).

We then quantified the spectral relationship between two timeseries, namely x (e.g. biophysical factors) and y (e.g. R_s), using cross-wavelet power

spectrum (C_n), phase angle spectrum (A_n), and WTC spectrum (R_n^2), which are defined, respectively, as:

$$C_n(s) = |W_n^{xy}(s)| = |W_n^x(s)W_n^{y*}(s)|, \quad (3)$$

$$A_n(s) = \tan^{-1} \left[\frac{\text{Im}(W_n^{xy}(s))}{\text{Re}(W_n^{xy}(s))} \right], \quad (4)$$

$$R_n^2(s) = \frac{|S(s^{-1}W_n^{xy}(s))|^2}{|S(s^{-1}W_n^x(s))|^2 |S(s^{-1}W_n^y(s))|^2}, \quad (5)$$

where W_n^{xy} is the XWT of x and y , S denotes a smoothing in time and scale, $\text{Im}[W_n^{xy}(s)]$ and $\text{Re}[W_n^{xy}(s)]$ are the imaginary and real part of $W_n^{xy}(s)$, respectively (Torrence and Compo 1998; Grinsted et al. 2004). The global cross-wavelet power spectrum (i.e. C_n averaged over time) quantifies the amount of covariance that occurs between two variables across a spectrum of frequencies (Vargas et al. 2010b). Phase angle spectrum (A_n) measures the time delay between x and y as a function of frequency, and can be drawn as arrows in the time-frequency space for C_n or R_n^2 . Arrows pointing downward indicate x leading y by 90° or lagging y by 270° , while arrows pointing upward indicate x lagging y by 90° or leading y by 270° . Arrows pointing right (left) indicate x and y vary in-phase (anti-phase), respectively. Wavelet coherence can be thought of as a measure of local correlation between two timeseries in the time-frequency domain (Grinsted et al. 2004; Vargas et al. 2010b). A statistically significant, phase-locked coherence provides an indication of causality (Koebsch et al. 2015). Moreover, phase angles can be used to infer possible causality between processes on the assumption that the effect must follow the cause (Vargas et al. 2010b). If more than one variable showed significant coherence with R_s at a given timescale, we considered the variable leading R_s by the smallest amount of time as the primary driving variable, assuming that a short response time is the best indicator of a close coupling between variables (Koebsch et al. 2015). We focused on WTC instead of XWT in examining biophysical controls on R_s , as WTC is considered a better measure of the interrelation between two variables than XWT (Grinsted et al. 2004; Vargas et al. 2010b). Global power spectra for XWT were included in the on-line supplementary material (Fig. S1).

Wavelet coherence between two timeseries, just like simple correlation, could be an artifact of common dependence on a third variable. Therefore, we further performed PWC, which can be considered the spectral counterpart of partial correlation (Ng and Chan 2012). The PWC spectrum (RP_n^2) is defined as:

$$RP_n^2(y, x_1, x_2) = \frac{|R_n(y, x_1) - R_n(y, x_2)R_n(y, x_1)|^2}{[1 - R_n(y, x_2)]^2 [1 - R_n(x_2, x_1)]^2}, \quad (6)$$

where RP_n^2 quantifies the coherence between y and x_1 after removing the effect of x_2 (Ng and Chan 2012). Both R_n^2 and RP_n^2 vary between 0 and 1, with values close to 1 indicating strong coherence between two timeseries.

All timeseries were normalized before wavelet analysis to have zero mean and unit variance. The statistical significance (at a 5% level) of wavelet spectra was tested using Monte Carlo methods against red noise (Grinsted et al. 2004; Vargas et al. 2010b). We focused only on areas outside the “cone-of-influence” (COI), in which the wavelet transform suffers from edge effects due to incomplete time-locality across frequencies (Vargas et al. 2012).

Because WTC is essentially a measure of local cross-correlation between two signals, it is most useful for inferring which causal linkages are possible (or impossible) on the assumptions mentioned above. Therefore, we further used the non-parametric spectral Granger-causality analysis, which enables a stronger indication of scale-specific causality between processes, to complement the results of WTC. Granger-causality is a method in which a timeseries x is said to have a causal linkage with another timeseries y , if x can be successfully used to predict the lagged response of y (Granger 1988; Hatala et al. 2012). Here we used a recent non-parametric spectral extension of the Granger-causality to the frequency domain (Detto et al. 2012) in identifying causal linkages between photosynthesis signals (i.e. GEP and PAR) and R_s and between T_s and R_s at the diel scale. Specifically, we used the conditional spectral Granger-causality, which allows for the differentiation of direct causal linkage from indirect linkage between multiple state variables, even under the influence of external drivers (Detto et al. 2012). In testing the statistical significance of an observed Granger-causality, 2000 random permutations were applied to the timeseries from which 95% confidence intervals were calculated around the null hypothesis (no Granger-

causality). Only growing-season data were used in the calculation of spectral Granger-causality because we focused on the relative effects of GEP and T_s in modulating R_s . Given the length of the dataset, the lowest and highest frequencies which can be resolved by the spectral Granger-causality analysis were 0.005 h^{-1} (a period of about 8 days) and 0.5 h^{-1} (a period of 2 h), respectively. This frequency range encompasses the 1-day period. Classic Granger-causality and its recent spectral extensions are described in full in Granger (1988) and Detto et al. (2012).

A caveat should be noted here that observational studies cannot fully resolve the causality between canopy photosynthesis and R_s , and that no algorithm can perfectly tease apart confounding factors in observational data. We aimed to take advantage of spectral techniques to reveal potential coupling or causal linkages between canopy photosynthesis and R_s across time-scales. The results of this study can provide testable hypotheses for manipulation or controlled experiments (e.g. clipping, trenching, and isotope labeling), which is a subject of our ongoing research.

We performed all analyses with MATLAB 7.11.0 (R2010b, The MathWorks, USA), using open source codes shared by Grinsted et al. (2004) and Ng and Chan (2012) for wavelet analyses, and those shared by Detto et al. (2012) for non-parametric spectral Granger-causality analyses. We focused mainly on three time-scales, i.e. the diel scale (1-day period), intermediate scales (from longer than 1-day to shorter than 200-day periods, with 200 days being about the growing-season length at our site), and seasonal to annual scales (200–365-day periods). The longest period which can be explored using wavelet analysis was about 444 days due to the limited length of our dataset. Therefore, quantifying interannual variations in R_s was not possible. It should be noted that timescales were classified in this way only to facilitate the interpretation of results, and variations in R_s and biophysical factors were essentially continuous in the time-frequency domain.

Results

Variations in R_s and biophysical factors

The semi-arid shrubland showed similar seasonal patterns in T_s and PAR across years during the study period (Fig. 1a). Daily mean T_s ranged from about

–10 °C in winter to 30 °C in summer. Photosynthetically active radiation had minimum values of <5 mol photons $\text{m}^{-2} \text{day}^{-1}$ on cloudy, winter days and maxima of 55–60 mol photons $\text{m}^{-2} \text{day}^{-1}$ on clear, mid-summer days. The annual rainfall was 278, 342, and 305 mm in 2013, 2014, and 2015, respectively. Rainfall showed a clear seasonal trend, with the growing-season (May–October) receiving 97, 84, and 77% of the annual total in 2013, 2014, and 2015, respectively (Fig. 1b). Soil water content at 10-cm depth varied seasonally from 0.05 to 0.12 $\text{m}^3 \text{m}^{-3}$, increasing abruptly in response to rainfall events and rapidly depleting during intervening dry periods (Fig. 1b). Low SWC during winter-time corresponded to frozen soil conditions as the sensors can only measure liquid water. Increases in SWC were thus observed in early spring when the soil underwent thawing.

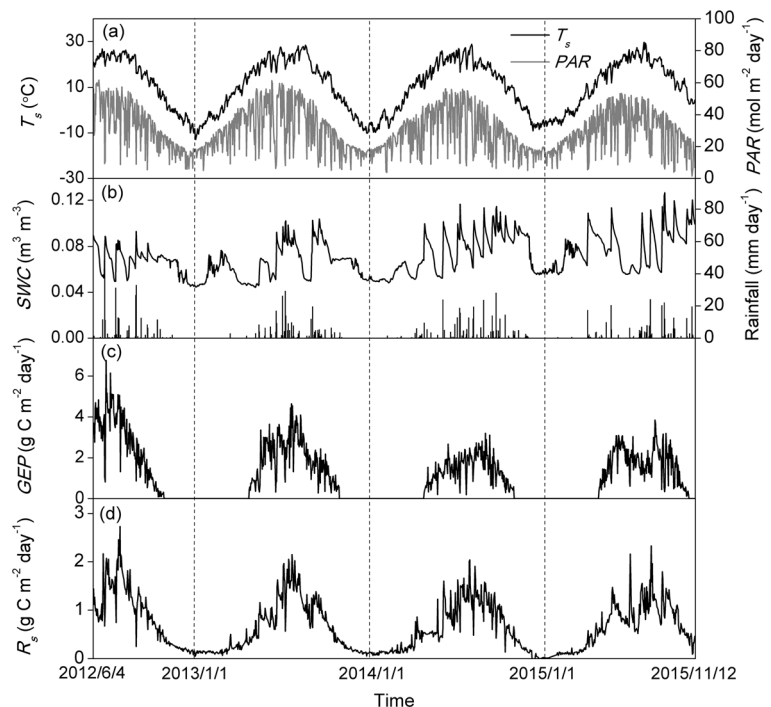
Maximum daily *GEP* was 6.51, 4.48, 3.09, and 3.71 $\text{g C m}^{-2} \text{day}^{-1}$ during each year of the study (Fig. 1c), and annual *GEP* was 361, 260, and 313 $\text{g C m}^{-2} \text{yr}^{-1}$ for 2013, 2014, and 2015, respectively. Daily R_s was lower than 0.10 $\mu\text{mol CO}_2 \text{m}^{-2} \text{s}^{-1}$ in winter, but reached seasonal maxima of 2.63, 2.07, 1.98, and 2.25 $\mu\text{mol CO}_2 \text{m}^{-2} \text{s}^{-1}$ during each

summer of the study (Fig. 1d). Annual R_s was 213 and 204 $\text{g C m}^{-2} \text{yr}^{-1}$ in 2013 and 2014, respectively (a large gap spanning 13 November 2015–26 February 2016 made a reliable annual R_s estimate impossible for the year 2015). Low SWC periods during the growing season generally corresponded to a depressed *GEP* and R_s (Fig. 1b–d).

Monthly mean diel variations showed that *PAR* and T_s peaked at about 13:00 and 16:00 (LST = GMT + 8), respectively, during the growing season (May–October; Fig. 2a and b). In contrast, both *GEP* and R_s increased rapidly during morning hours and tended to peak before mid-noon, especially during the mid-growing season (Jun–August; Fig. 2c and d).

According to the global wavelet power spectra (Fig. 3), all timeseries examined were characterized by high variability (periodicity) at the diel and seasonal to annual timescales. Soil water content showed the highest variability at intermediate temporal scales (i.e. days, weeks and months) among the timeseries examined. Local wavelet power spectra (Fig. S2) for all examined variables were consistent with their spectral peaks in global power spectra.

Fig. 1 Seasonal variation in **a** daily mean soil temperature at a 10-cm depth (T_s) and daily-integrated photosynthetically active radiation (*PAR*), **b** volumetric soil water content at a 10-cm depth (*SWC*) and rainfall, **c** daily gross ecosystem productivity (*GEP*) and **d** daily soil respiration (R_s) from 3 June, 2012 to 12 November, 2015. Vertical dashed lines are used to separate the data according to year; environmental factors and *GEP* for 2012–2014 have been previously reported by Jia et al. (2014, 2016)



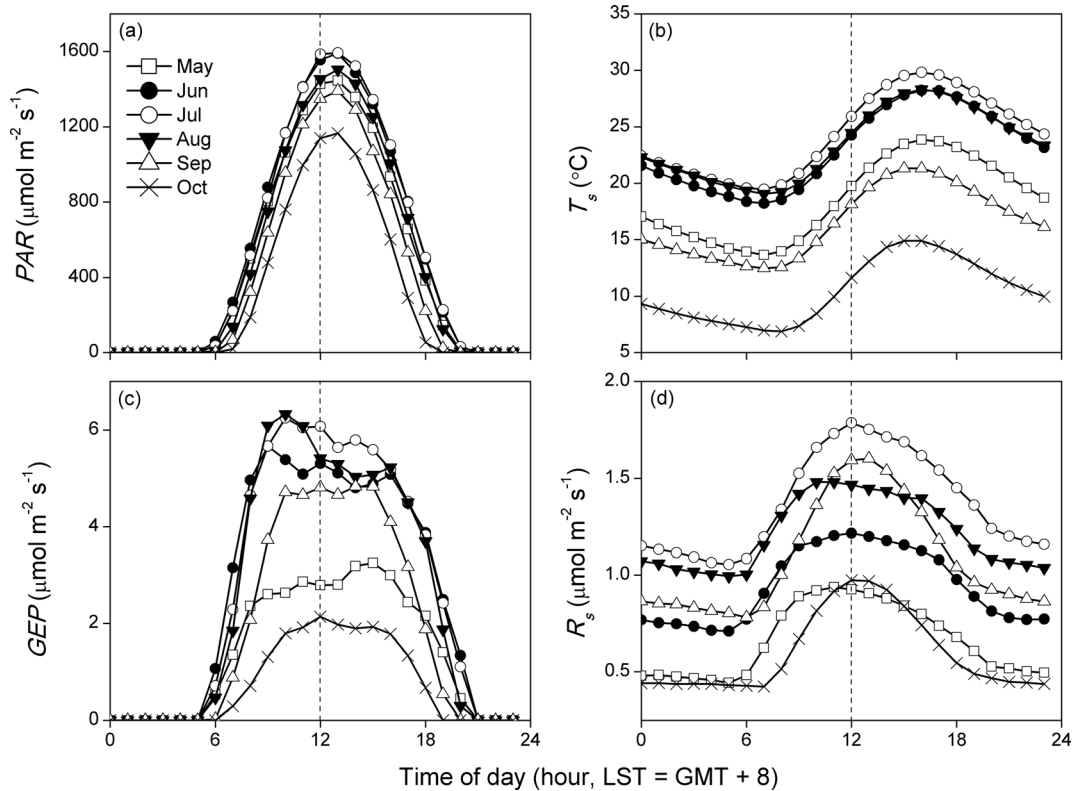


Fig. 2 Mean diel variation in **a** photosynthetically active radiation (*PAR*), **b** soil temperature at a 10-cm depth (T_s), **c** gross ecosystem productivity (*GEP*) and **d** soil respiration (R_s) for each month of

the growing season (May–October). Vertical dashed-lines denote mid-noon (i.e. 12:00, LST = GMT + 8)

Relationships between R_s and biophysical factors at the diel scale

Significant WTC was observed between R_s and *GEP* at the 1-day scale during the growing season (Fig. 4a). Wavelet coherence also showed that R_s was tightly correlated with *PAR* and T_s at the diel scale over most of the observation period (Fig. 4b and c) and with *SWC* during some non-continuous time periods (Fig. 4d). Diel variations in R_s were mostly in-phase with variations in *GEP* and *PAR* (i.e. arrows pointing right, Fig. 4a and b). The phase angle between R_s and *GEP* was $3.74 \pm 18.66^{\circ}$ (mean \pm standard deviation) at the 1-day period, i.e. R_s lagged *GEP* by 0.25 ± 1.24 h (Figs. 4a and 5a). The diel phase angle between R_s and *PAR* was $-0.42 \pm 29.13^{\circ}$, i.e. a negligible time lag of 0.03 ± 1.94 h (Figs. 4b and 5a). In contrast, the phase angles for R_s – T_s and R_s –*SWC* relationships were $-67.53 \pm 32.16^{\circ}$ (R_s leading T_s by 4.50 ± 2.14 h) and $-81.48 \pm 36.00^{\circ}$ (R_s leading *SWC* by 5.43 ± 2.40 h), respectively (Figs. 4c, d and 5a). Partial wavelet coherence between R_s and biophysical

factors was generally weak over the 1-day period, except for that between R_s and T_s during the non-growing seasons after removing the effects of the other factors on R_s (Fig. S3). The Granger-causality spectra for the effects of both *GEP* and T_s on R_s showed a strong peak at the diel scale (frequency of about 0.04 h^{-1} , Fig. 6), and the diel peak for *GEP* effects remained significant after removing the effects of T_s on R_s (Fig. 6a). In contrast, the diel peak for T_s effects became insignificant after removing the effects of *GEP* on R_s (Fig. 6b). There was also a spectral peak at about 0.1 h^{-1} (i.e. 10-h period) for the Granger-causality between R_s and T_s (Fig. 6b).

Relationships between R_s and biophysical factors at intermediate scales

Non-continuous areas of significant WTC were observed between R_s and biophysical factors over a wide range of timescales (Fig. 4). Firstly, photosynthesis-related factors (*GEP* and *PAR*) showed coherence with R_s over 8–64-day periods

Fig. 3 Global wavelet power spectra for gross ecosystem productivity (GEP), photosynthetically active radiation (PAR), soil temperature and water content at a 10-cm depth (T_s and SWC , respectively) and soil respiration (R_s)

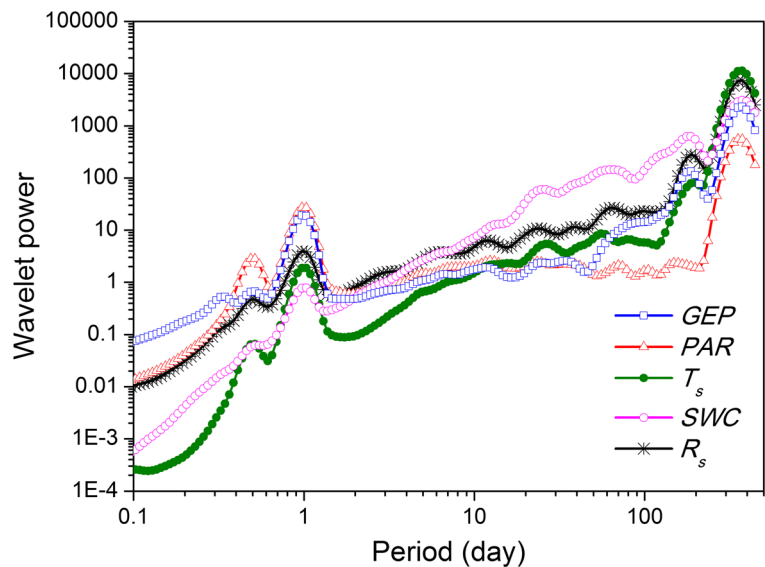


(Fig. 4a and b, S3a–c), although the effects of PAR were greatly weakened when the influences of other factors on R_s were removed (Fig. S3d–f). Secondly, R_s was correlated with T_s over 1–16-day periods during the non-growing seasons (Figs. 4b, S3g–i). Thirdly, hotspots of WTC and PWC were found between R_s and SWC over 4–64-day periods (Figs. 4d, S3j–l). In particular, both GEP and SWC showed strong WTC with R_s over 32–64-day periods over the growing season of 2013, the year with the lowest annual rainfall during the observation period. The Granger-causality for the R_s – T_s relationship showed a spectral peak at about 0.01 h^{-1} (i.e. 100-h period, Fig. 6b).

Relationships between R_s and biophysical factors at seasonal to annual scales

Soil respiration was positively correlated with GEP (Fig. S4a, b), and increased exponentially with T_s (Fig. S4c, d) over the study period. Significant WTC was found between R_s and all examined biophysical factors at seasonal to annual timescales over the study period (Fig. 4). Soil respiration oscillated nearly in phase with GEP at the 1-year scale (i.e. arrows pointing right, Fig. 4a), but out of phase with other factors (i.e. arrows pointing in other directions, Fig. 4b–d). The phase angle between R_s and GEP was $2.47 \pm 0.23^\circ$ over an annual timescale, i.e. R_s lagged GEP by about 2.5 days (Fig. 5b). In contrast, the phase angles for R_s – PAR , R_s – T_s , and R_s – SWC relationships were $34.45 \pm 0.49^\circ$, 16.65

$\pm 0.08^\circ$, and 25.07 ± 1.54 , respectively. Specifically, R_s lagged PAR and T_s by about 35 and 16 days, respectively, and led SWC by about 25 days (Fig. 5b). Significant PWC was observed between GEP and R_s at seasonal to annual scales after removing the effects of the other factors on R_s (Fig. S3a–c). However, PWC was less robust between R_s and other factors at these timescales (Fig. S3d–l).

Discussion

Effects of photosynthesis on R_s at the diel timescale

Our results showed that R_s was closely coupled with canopy photosynthesis (GEP and PAR) at the diel scale (Figs. 4a, b and 5a). In contrast, R_s preceded both T_s and SWC by several hours (Figs. 4c, d and 5a), indicating that soil physical factors were not the primary drivers of R_s dynamics at the diel scale. The diel variation in R_s followed that in GEP with a negligible time lag ($0.25 \pm 1.24 \text{ h}$) during the growing seasons (Figs. 4 and 5). This finding is consistent with previous studies which documented nearly in-phase linkages between photosynthetic activity and R_s in different ecosystems (see Table 1 for a summary of the literature). On the contrary, other studies observed time lags ranging from a few to more than 10 h between assimilation and respiration at the diel scale (Table 1). One mechanism responsible for the time lag between photosynthesis and R_s

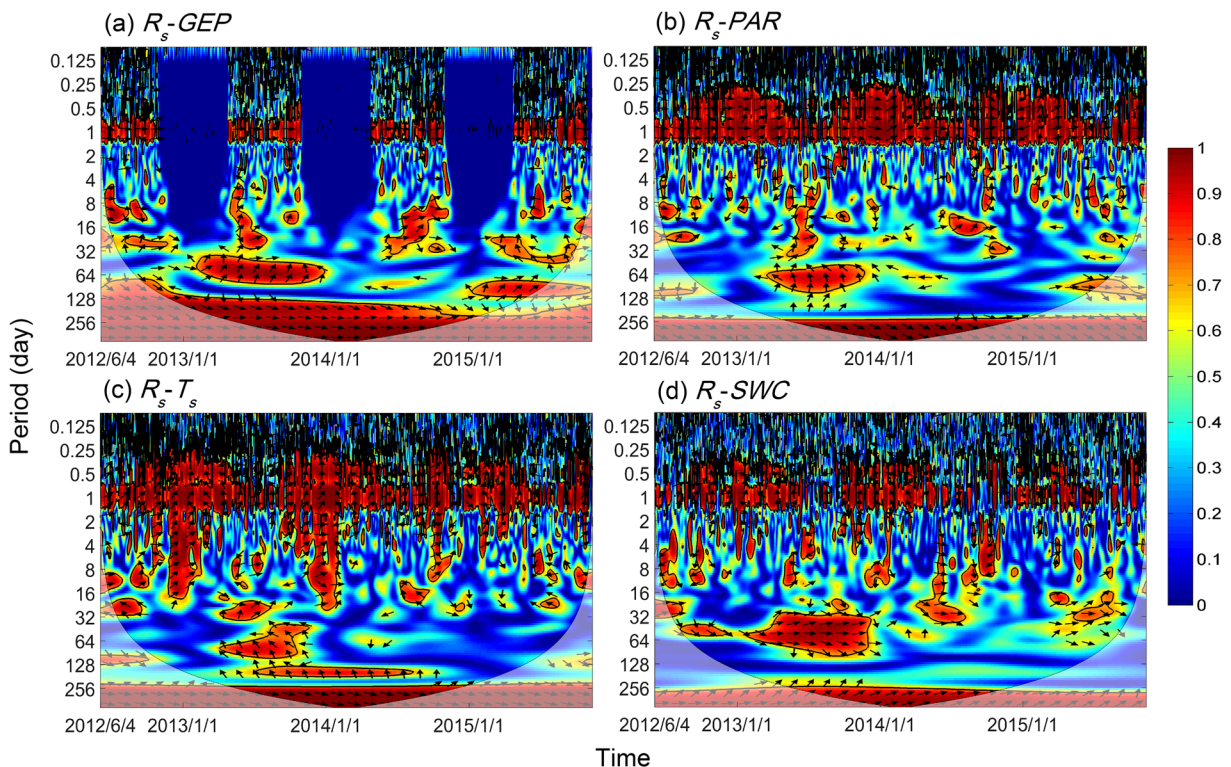


Fig. 4 Wavelet coherence between soil respiration (R_s) and **a** gross ecosystem productivity (GEP), **b** photosynthetically active radiation (PAR) and **c**, **d** soil temperature and water content at a 10-cm depth (SWC). The arrows show the phase difference. Arrows pointing upward indicate biophysical factors lagging R_s by 90° or leading R_s by 270° , while arrows pointing downward indicate

biophysical factors leading R_s by 90° or lagging R_s by 270° . Arrows pointing right or left indicate that biophysical factors and R_s vary in-phase or out-of-phase (anti-phase), respectively. Black contour lines represent the 0.05 significance level and the thin lines indicate the cone-of-influence that delimits the region not influenced by edge effects

is the transport of photosynthetic products from the canopy to the rhizosphere by way of the phloem (Högberg et al. 2001, 2008; Mencuccini and Hölttä 2010). Based on this mechanism, photo-assimilates should be transported over a shorter distance in short than high plants, resulting in much shorter time lags observed in shrublands and grasslands, than in forests (Kuzyakov and Gavrichkova 2010; Mencuccini and Hölttä 2010). The short canopy at our site (0.5–1.0 m) thus may partially explain the rapid coupling between GEP and R_s .

Another mechanism underlying the time lag is associated with the loading of new assimilates into the phloem and subsequent propagation of turgor and osmotic-pressure waves from leaves to roots (i.e. pressure-concentration waves; Mencuccini and Hölttä 2010). Accordingly, pressure waves, rather than molecules of new assimilates, are transferred belowground (Kuzyakov and Gavrichkova 2010). Pressure-concentration waves move much faster down the

phloem than molecules of new assimilates, and thus could possibly lead to nearly in-phase coupling between photosynthesis and R_s (Kuzyakov and Gavrichkova 2010). The fast propagation of pressure-concentration waves could thus be another important explanation for the observed synchrony between photosynthesis proxies and R_s at the diel scale (Barba et al. 2018; Liu et al. 2006; Vargas et al. 2011).

Short time lags also indicate that recent assimilates may be quickly consumed, i.e. with little transitory storage and later remobilization at the diel scale (Han et al. 2014; Liu et al. 2006). This may be the case in semi-arid vegetation due to frequent drought stress and a large investment of assimilates in the maintenance of physiological activity (Kuzyakov and Gavrichkova 2010). In addition, the short time lag found here may also be partially attributable to the well-aerated sandy soil and relatively shallow rooting depth of the dominant species (fine roots are mainly distributed in the 20–50 cm layer, Jia et al. 2016), both reducing the path length time for CO_2 to diffuse from the

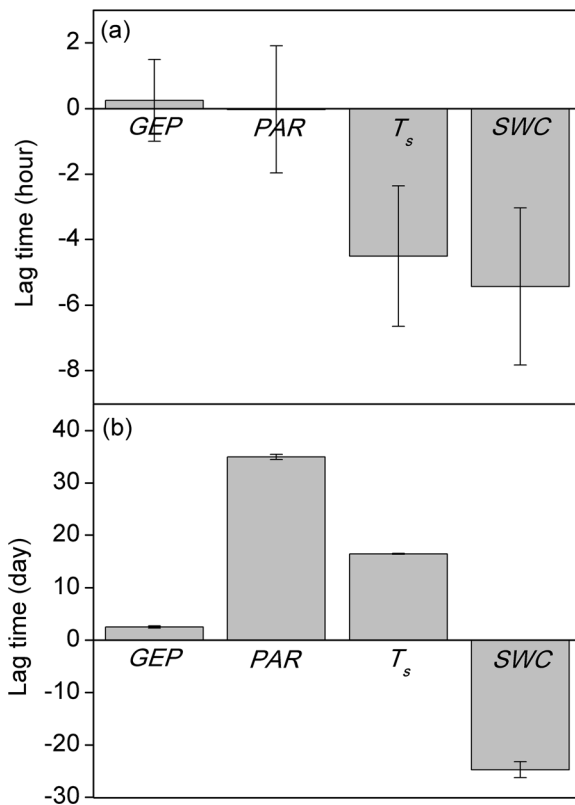


Fig. 5 Time lags between soil respiration (R_s) and biophysical factors at **a** diel and **b** annual timescales. *GEP* stands for gross ecosystem productivity; *PAR*, photosynthetically active radiation; T_s , soil temperature; and *SWC*, soil water content at a 10-cm depth. Positive values indicate that R_s lags biophysical factors, whereas negative values indicate an opposite trend. Data represent mean \pm standard deviation

main rooting zone to the soil surface (typically 0.12–0.75 h, estimated following Martin et al. 2012). Future studies should examine the relative importance of different mechanisms in determining the time lag between photosynthesis and R_s .

The time lag of about 4.5 h between R_s and T_s at the diel scale (Fig. 4b) was comparable to those reported for other ecosystems (e.g. Carbone et al. 2008; Han et al. 2014; Vargas et al. 2010b, 2011). Diel phase lags between R_s and T_s can result from: (1) a mismatch between the depth of temperature measurements and that of CO_2 production, (2) the time needed for the diffusion of gas from the soil complex to the atmosphere, or (3) the regulation of diel variations in R_s by photosynthetic substrate supply (Jia et al. 2013; Martin et al. 2012; Phillips et al. 2011). The first explanation is unlikely to be applicable here, due to the fact that T_s was measured at a shallow depth (10 cm), where heat transfer

should be technically faster, and that T_s lagged R_s by several hours. Diffusion of CO_2 upward is expected to result in an opposite pattern, i.e. T_s leading R_s . Hence, plant photosynthesis, which varied out-of-phase with T_s at the diel scale (Fig. 2b and c), may have modulated the diel variations in R_s and thus played a major role in decoupling T_s from R_s .

Effects of photosynthesis on R_s at intermediate timescales

Our finding that photosynthesis proxies (*GEP* and *PAR*) showed localized temporal correlations with R_s at timescales of days to months (Fig. 4a, b and S3a–c) agrees with previous studies in semi-arid ecosystems (Vargas et al. 2010b, 2011, 2012), and supports our hypothesis that photosynthetic substrate supply could affect R_s dynamics at intermediate timescales. Changes in canopy photosynthesis driven by weather patterns (e.g. rain events, droughts, heat waves, and cold spells) could mediate environmental effects on R_s (Heinemeyer et al. 2012; Wang et al. 2014). We observed that R_s was temporally correlated with both *GEP* and *SWC* over 32–64-day periods during the growing season of 2013 (Fig. 4a and d), the year with the lowest annual rainfall. This indicates that soil water deficit may constrain R_s through depressed plant photosynthetic activity and subsequently reduced assimilate supply to roots and the rhizosphere (Barba et al. 2018; Heinemeyer et al. 2012; Vargas et al. 2012). In line with our results, increases in soil moisture have been found to significantly enhance plant photosynthetic rates and below-ground C allocation, stimulating both root and microbial respiration in semi-arid steppes (Liu et al. 2009; Yan et al. 2011). In addition, photosynthetic signatures in R_s at intermediate timescales could also be associated with the dynamics of plant carbohydrate reserves that feature different turnover rates (Carbone and Trumbore 2007; Heinemeyer et al. 2012; Mencuccini and Hölttä 2010). It is noteworthy that despite clear localized temporal correlations between *GEP* and R_s at intermediate scales, T_s may also affect R_s at timescales of days to weeks (Figs. 4, 6b, and S3).

Effects of photosynthesis on R_s at seasonal to annual timescales

Primary production is an important driver of soil CO_2 fluxes not only over short timescales (i.e. hours to days),

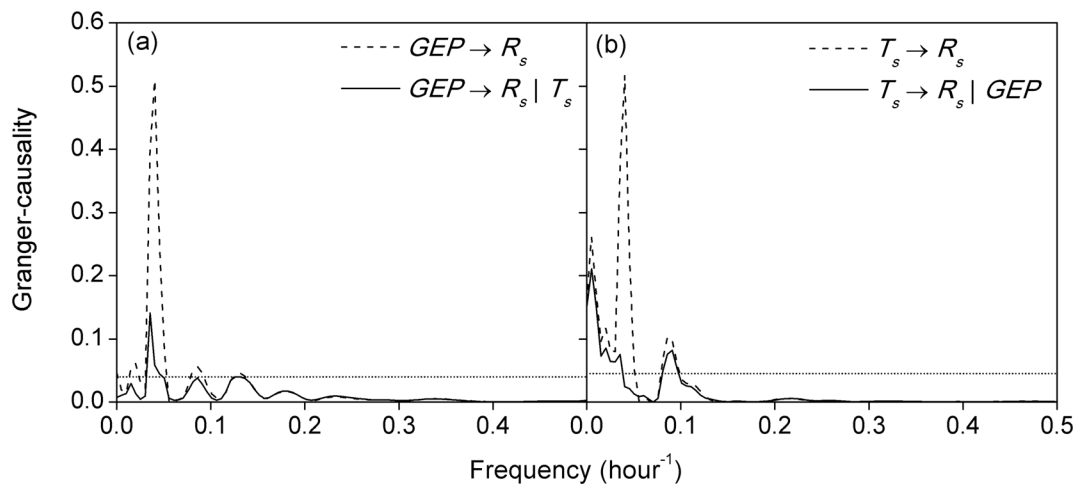


Fig. 6 Granger-causality spectra for **a** gross ecosystem productivity (GEP) and **b** soil temperature at a 10-cm depth (T_s) with respect to soil respiration (R_s). Dashed curves are for the spectral Granger-causality and solid curves for the conditional spectral

Granger-causality. Data for the June–September period were used in this analysis. Dotted lines represent 95% confidence intervals around the null hypothesis (no Granger-causality), obtained by applying random permutations to tested timeseries 2000 times

but also on seasonal to annual scales (Bahn et al. 2008; Kuzyakov and Gavrichkova 2010). Although R_s in this study showed temporal correlation with all examined biophysical factors at seasonal to annual scales (Fig. 4), the coherence between GEP and R_s was strongest, as revealed by PWC (Fig. S3). The observation that R_s preceded SWC at seasonal to annual timescales (Figs. 4d, and 5b) indicates that SWC was not the main factor controlling seasonal variations in R_s . Moreover, R_s lagged GEP by only 2 days at seasonal to annual timescales, but lagged PAR and T_s by many more days (Fig. 5b). These findings support a stronger coupling between R_s and GEP , than between R_s and other factors. In

addition, the seasonality of GEP (i.e. canopy phenology) seemed to lag seasonal variations in PAR and T_s (Fig. 5b), and thus might have decoupled R_s from seasonal changes in radiation and temperature. Similar to our results, seasonal dynamics of R_s was observed to be nearly in-phase with GEP in European grasslands (Vargas et al. 2010a). In a mixed temperate forest, the seasonal peak in basal R_s rates coincided with that of GEP , whereas temperature peaked 6 weeks later (Sampson et al. 2007). In addition, previous studies have demonstrated that GEP , rather than T_s , determined annual R_s in forests (Janssens et al. 2001; Vargas et al. 2010a), shrublands (Reichstein et al. 2003), and

Table 1 Time lag between photosynthesis and R_s at the diel scale reported here and in the literature

Location	Ecosystem type	Time lag (h)	Reference
Northern China	Temperate semi-arid shrubland	0.25 ± 1.24	This study
NE Iberian Peninsula	Mixed Mediterranean forest	Almost no lags	Barba et al. (2018)
Austria	Temperate grassland	0.9 ± 3.9	Vargas et al. (2011)
Southeastern U.S.	Sweetgum forest	1	Liu et al. (2006)
East China	Coastal wetland	1–1.5	Han et al. (2014)
Cross-site synthesis	Grasslands	12.5 ± 7.5	Kuzyakov and Gavrichkova (2010)
CA, USA	Mediterranean deciduous woodland	3.0 ± 1.1	Vargas et al. (2011)
Central Missouri, USA	Temperate broadleaf forest	7.6 ± 2.4	Vargas et al. (2011)
Finland	Boreal evergreen forest	4.0 ± 0.8	Vargas et al. (2011)
CA, USA	Oak-grass savanna	7–12	Tang et al. (2005)
SE England	Temperate deciduous oak forest	11 ± 3	Heinemeyer et al. (2012)

grasslands (Bahn et al. 2008). In contrast, some studies reported seasonal time lags ranging from a few days to a few weeks for R_s in forest ecosystems to respond to seasonal variations in photosynthetic production (Baldocchi et al. 2006; Gaumont-Guay et al. 2008; Martin et al. 2012; Vargas et al. 2010a). Although transport distance (e.g. canopy height plus rooting depth) can affect the speed of linkage between photosynthesis and R_s (Mencuccini and Hölttä 2010), seasonal lags between these two processes also depend on plant C allocation to above- vs. belowground tissues and to storage vs. immediate use (Carbone and Trumbore 2007; Kuzyakov and Gavrichkova 2010). Short time lags between photosynthesis and R_s at seasonal to annual timescales (Figs. 4a and 5b) suggest rapid allocation and use of C in root and rhizosphere respiration.

Conclusions

By applying spectral analyses to long-term continuous CO_2 flux measurements, we showed that variations in R_s were closely linked with those in GEP at diel and seasonal to annual timescales. Furthermore, non-continuous areas of high WTC were also found between R_s and GEP at timescales of days to months. These results indicate that photosynthetic production may play an important role in modulating R_s in the shrubland ecosystem at multiple timescales. Therefore, ecosystem C models need to explicitly consider different mechanisms by which current or recent assimilates drive soil and ecosystem respiration. This study also illustrates the need for a multi-scale approach to understanding the temporal dynamics of C fluxes. We suggest that future studies combine field manipulations (e.g. trenching, girdling, clipping, and isotope labeling) with spectral analysis for a more mechanistic understanding of the coupling between photosynthesis and R_s .

Acknowledgements This study was funded by the National Natural Science Foundation of China (NSFC, grant numbers 31670708 and 31670710), the Fundamental Research Funds for the Central Universities (grant number 2015ZCQ-SB-02), and the National Key Research and Development Program of China (grant number 2016YFC0500905). This work was also promoted by the U.S.–China Carbon Consortium (USCCC). We thank X. W. Yang, S. J. Liu, G. P. Chen, and C. Zhang for their assistance with field measurements and instrumentation maintenance. We also thank J. J. Zheng for proofreading the manuscript.

References

- Bahn M, Rodeghiero M, Anderson-Dunn M, Dore S, Gimeno C, Drösler M, Williams M, Ammann C, Berninger F, Flechard C, Jones S, Balzarolo M, Kumar S, Newesely C, Priwitzer T, Raschi A, Siegwolf R, Susiluoto S, Tenhunen J, Wohlfahrt G, Cernusca A (2008) Soil respiration in European grasslands in relation to climate and assimilate supply. *Ecosystems* 11: 1352–1367. <https://doi.org/10.1007/s10021-008-9198-0>
- Bahn M, Schmitt M, Siegwolf R, Richter A, Brüggemann N (2009) Does photosynthesis affect grassland soil-respired CO_2 and its carbon isotope composition on a diurnal timescale? *New Phytol* 182:451–460. <https://doi.org/10.1111/j.1469-8137.2008.02755.x>
- Baldocchi D, Tang J, Xu L (2006) How switches and lags in biophysical regulators affect spatial-temporal variation of soil respiration in an oak-grass savanna. *J Geophys Res* 111:G02008. <https://doi.org/10.1029/2005JG000063>
- Barba J, Lloret F, Poyatos R, Molowny-Horas R, Curiel Yuste L (2018) Multi-temporal influence of vegetation on soil respiration in a drought-affected forest. *iForest* 11:189–198. <https://doi.org/10.3832/ifor2448-011>
- Barron-Gafford GA, Scott RL, Jenerette GD, Huxman TE (2011) The relative controls of temperature, soil moisture, and plant functional group on soil CO_2 efflux at diel, seasonal, and annual scales. *J Geophys Res* 116:G01023. <https://doi.org/10.1029/2010JG001442>
- Bond-Lamberty B, Thomson A (2010) Temperature-associated increases in the global soil respiration record. *Nature* 464: 579–582. <https://doi.org/10.1038/nature08930>
- Carbone MS, Trumbore SE (2007) Contribution of new photosynthetic assimilates to respiration by perennial grasses and shrubs: residence times and allocation patterns. *New Phytol* 176:124–135. <https://doi.org/10.1111/j.1469-8137.2007.02153.x>
- Carbone MS, Winston GC, Trumbore SE (2008) Soil respiration in perennial grass and shrub ecosystems: linking environmental controls with plant and microbial sources on seasonal and diel timescales. *J Geophys Res* 113:G02022. <https://doi.org/10.1029/2007JG000611>
- Cazelles B, Chavez M, Berteaux D, Ménard F, Olav Vik J, Jenouvrier S, Stenseth NC (2008) Wavelet analysis of ecological time series. *Oecologia* 156:287–304. <https://doi.org/10.1007/s00442-008-0993-2>
- Detto M, Molini A, Katul G, Stoy P, Palmroth S, Baldocchi D (2012) Causality and persistence in ecological systems: a nonparametric spectral granger causality approach. *Am Nat* 179:524–535. <https://doi.org/10.1086/664628>
- Falge E, Baldocchi D, Olson R, Anthoni P, Aubinet M, Bernhofer C, Burba G, Ceulemans R, Clement R, Dolman H, Grainier A, Gross P, Grünwald T, Hollinger D, Jensen N-O, Katul G, Keronen P, Kowalski A, Lai CT, Law BE, Meyers T, Moncrieff J, Moors E, Munger JW, Pilegaard K, Rannik Ü, Rebmann C, Suyker A, Tenhunen J, Tu K, Verma S, Vesala T, Wilson K, Wofsy S (2001) Gap filling strategies for defensible annual sums of net ecosystem exchange. *Agric For Meteorol* 107:43–69. [https://doi.org/10.1016/S0168-1923\(00\)00225-2](https://doi.org/10.1016/S0168-1923(00)00225-2)
- Feng W, Zhang Y, Jia X, Wu B, Zha T, Qin S, Wang B, Shao C, Liu J, Fa K (2014) Impact of environmental factors and biological soil crust types on soil respiration in a desert ecosystem. *PLoS One* 9: e102954. <https://doi.org/10.1371/journal.pone.0102954>

- Gaumont-Guay D, Black TA, Barr AG, Jassal R, Nesic Z (2008) Biophysical controls on rhizospheric and heterotrophic components of soil respiration in a boreal black spruce stand. *Tree Physiol* 28:161–171. <https://doi.org/10.1093/treephys/28.2.161>
- Granger CW (1988) Some recent developments in the concept of causality. *J Econ* 39:199–211. [https://doi.org/10.1016/0304-4076\(88\)90045-0](https://doi.org/10.1016/0304-4076(88)90045-0)
- Grinsted A, Moore JC, Jevrejeva S (2004) Application of the cross wavelet transform and wavelet coherence to geophysical time series. *Nonlinear Process Geophys* 11:561–566. <https://doi.org/10.5194/npg-11-561-2004>
- Han G, Luo Y, Li D, Xia J, Xing Q, Yu J (2014) Ecosystem photosynthesis regulates soil respiration on a diurnal scale with a short-term time lag in a coastal wetland. *Soil Biol Biochem* 68: 85–94. <https://doi.org/10.1016/j.soilbio.2013.09.024>
- Hatala JA, Detto M, Baldocchi DD (2012) Gross ecosystem photosynthesis causes a diurnal pattern in methane emission from rice. *Geophys Res Lett* 39:L06409. <https://doi.org/10.1029/2012GL051303>
- Heinemeyer A, Wilkinson M, Vargas R, Subke J-A, Casella E, Morison JIL, Ineson P (2012) Exploring the “overflow tap” theory: linking forest soil CO₂ fluxes and individual mycorrhizosphere components to photosynthesis. *Biogeosciences* 9:79–95. <https://doi.org/10.5194/bg-9-79-2012>
- Högberg P, Nordgren A, Buchmann N, Taylor AFS, Ekblad A, Högberg MN, Nyberg G, Ottosson-Löfvenius M, Read DJ (2001) Large-scale forest girdling shows that current photosynthesis drives soil respiration. *Nature* 411:789–792. <https://doi.org/10.1038/35081058>
- Högberg P, Högberg MN, Göttlicher SG, Betson NR, Keel SG, Metcalfe DB, Campbell C, Schindlbacher A, Hurry V, Lundmark T, Linder S, Näsholm T (2008) High temporal resolution tracing of photosynthate carbon from the tree canopy to forest soil microorganisms. *New Phytol* 177: 220–228. <https://doi.org/10.1111/j.1469-8137.2007.02238.x>
- Högberg P, Singh B, Löfvenius MO, Nordgren A (2009) Partitioning of soil respiration into its autotrophic and heterotrophic components by means of tree-girdling in old boreal spruce forest. *For Ecol Manag* 257:1764–1767. <https://doi.org/10.1016/j.foreco.2009.01.036>
- Janssens IA, Lankreijer H, Matteucci G, Kowalski AS, Buchmann N, Epron D, Pilegaard K, Kutsch W, Longdoz B, Grünwald T, Grelle A, Rannik Ü, Morgenstern K, Oltchev S, Clement R, Gudmundsson J, Minerbi S, Berbigier P, Ibrom A, Moncrieff J, Aubinet M, Bernhofer C, Jensen NO, Vesala T, Granier A, Schulze D, Lindroth A, Dolman AJ, Jarvis PG, Ceulemans R, Valentini R (2001) Productivity overshadows temperature in determining soil and ecosystem respiration across European forests. *Glob Chang Biol* 7:269–278. <https://doi.org/10.1046/j.1365-2486.2001.00412.x>
- Jia X, Zha T, Wu B, Zhang Y, Chen W, Wang X, Yu H, He G (2013) Temperature response of soil respiration in a Chinese pine plantation: hysteresis and seasonal vs. diel Q₁₀. *PLoS One* 8: e57858. <https://doi.org/10.1371/journal.pone.0057858>
- Jia X, Zha TS, Wu B, Zhang YQ, Gong JN, Qin SG, Chen GP, Qian D, Kellomäki S, Peltola H (2014) Biophysical controls on net ecosystem CO₂ exchange over a semi-arid shrubland in northwest China. *Biogeosciences* 11:4679–4693. <https://doi.org/10.5194/bg-11-4679-2014>
- Jia X, Zha T, Gong J, Wang B, Zhang Y, Wu B, Qin S, Peltola H (2016) Carbon and water exchange over a temperate semi-arid shrubland during three years of contrasting precipitation and soil moisture patterns. *Agric For Meteorol* 228:120–129. <https://doi.org/10.1016/j.agrformet.2016.07.007>
- Koebisch F, Jurasinski G, Koch M, Hofmann J, Clatzel S (2015) Controls for multi-scale temporal variation in ecosystem methane exchange during the growing season of a permanently inundated fen. *Agric For Meteorol* 204:94–105. <https://doi.org/10.1016/j.agrformet.2015.02.002>
- Kuzyakov Y, Gavrichkova O (2010) Time lag between photosynthesis and carbon dioxide efflux from soil: a review of mechanisms and controls. *Glob Chang Biol* 16:3386–3406. <https://doi.org/10.1111/j.1365-2486.2010.02179.x>
- Liu Q, Edwards NT, Post WM, Gu L, Ledford J, Lenhart S (2006) Temperature-independent diel variation in soil respiration observed from a temperate deciduous forest. *Glob Chang Biol* 12: 2136–2145. <https://doi.org/10.1111/j.1365-2486.2006.01245.x>
- Liu W, Zhang Z, Wan S (2009) Predominant role of water in regulating soil and microbial respiration and their responses to climate change in a semi-arid grassland. *Glob Chang Biol* 15:184–195. <https://doi.org/10.1111/j.1365-2486.2008.01728.x>
- Luo Y (2007) Terrestrial carbon-cycle feedback to climate warming. *Annu Rev Ecol Evol Syst* 38:683–712. <https://doi.org/10.1146/annurev.ecolsys.38.091206.095808>
- Luo Y, Zhou X (2006) Soil respiration and the environment. Academic Press/Elsevier, San Diego
- Martin JG, Phillips CL, Schmidt A, Irvine J, Law BE (2012) High-frequency analysis of the complex linkage between soil CO₂ fluxes, photosynthesis and environmental variables. *Tree Physiol* 32:49–64. <https://doi.org/10.1093/treephys/tp134>
- Mencuccini M, Hölttä T (2010) The significance of phloem transport for the speed with which canopy photosynthesis and belowground respiration are linked. *New Phytol* 185:189–203. <https://doi.org/10.1111/j.1469-8137.2009.03050.x>
- Ng EKW, Chan JCL (2012) Geophysical applications of partial wavelet coherence and multiple wavelet coherence. *J Atmos Ocean Technol* 29:1845–1853. <https://doi.org/10.1175/JTECH-D-12-00056.1>
- Phillips CL, Nickerson N, Risk D, Bond BJ (2011) Interpreting diel hysteresis between soil respiration and temperature. *Glob Chang Biol* 17:515–527. <https://doi.org/10.1111/j.1365-2486.2010.02250.x>
- Reichstein M, Rey A, Freibauer A, Tenhunen J, Valentini R, Banza J, Casals P, Cheng Y, Grünzweig JM, Irvine J, Joffre R, Law BE, Loustau D, Miglietta F, Oechel W, Ourcival J-M, Pereira JS, Peressotti A, Ponti F, Qi Y, Rambal S, Rayment M, Romanya J, Rossi F, Tedeschi V, Tirone G, Xu M, Yakir D (2003) Modeling temporal and large-scale spatial variability of soil respiration from soil water availability, temperature and vegetation productivity indices. *Glob Biogeochem Cycles* 17:1104. <https://doi.org/10.1029/2003GB002035>
- Sampson DA, Janssens IA, Curiel Yuste J, Ceulemans R (2007) Basal rates of soil respiration are correlated with photosynthesis in a mixed temperate forest. *Glob Chang Biol* 13:2008–2017. <https://doi.org/10.1111/j.1365-2486.2007.01414.x>
- Savage K, Davidson EA, Tang J (2013) Diel patterns of autotrophic and heterotrophic respiration among phenological stages. *Glob Chang Biol* 19:1151–1159. <https://doi.org/10.1111/gcb.12108>
- Tang J, Baldocchi DD, Xu L (2005) Tree photosynthesis modulates soil respiration on a diurnal time scale. *Glob Chang Biol* 11: 1298–1304. <https://doi.org/10.1111/j.1365-2486.2005.00978.x>

- Torrence C, Compo GP (1998) A practical guide to wavelet analysis. *Bull Am Meteorol Soc* 79:61–78. [https://doi.org/10.1175/1520-0477\(1998\)079<0061:APGTWA>2.0.CO;2](https://doi.org/10.1175/1520-0477(1998)079<0061:APGTWA>2.0.CO;2)
- Vargas R, Baldocchi DD, Allen MF, Bahn M, Black TA, Collins SL, Curiel Yuste J, Hirano T, Jassal RS, Pumpanen J, Tang J (2010a) Looking deeper into the soil: biophysical controls and seasonal lags of soil CO₂ production and efflux. *Ecol Appl* 20:1569–1582. <https://doi.org/10.1890/09-0693.1>
- Vargas R, Detto M, Baldocchi DD, Allen MF (2010b) Multiscale analysis of temporal variability of soil CO₂ production as influenced by weather and vegetation. *Glob Chang Biol* 16:1589–1605. <https://doi.org/10.1111/j.1365-2486.2009.02111.x>
- Vargas R, Baldocchi DD, Bahn M, Hanson PJ, Hosman KP, Kulmala L, Pumpanen J, Yang B (2011) On the multi-temporal correlation between photosynthesis and soil CO₂ efflux: reconciling lags and observations. *New Phytol* 191:1006–1017. <https://doi.org/10.1111/j.1469-8137.2011.03771.x>
- Vargas R, Collins SL, Thomey ML, Johnson JE, Brown RF, Natvig DO, Friggens MT (2012) Precipitation variability and fire influence the temporal dynamics of soil CO₂ efflux in an arid grassland. *Glob Chang Biol* 18:1401–1411. <https://doi.org/10.1111/j.1365-2486.2011.02628.x>
- Wang B, Zha TS, Jia X, Wu B, Zhang YQ, Qin SG (2014) Soil moisture modifies the response of soil respiration to temperature in a desert shrub ecosystem. *Biogeosciences* 11:259–268. <https://doi.org/10.5194/bg-11-259-2014>
- Wang B, Zha TS, Jia X, Gong JN, Wu B, Bourque CPA, Zhang Y, Qin SG, Chen GP, Peltola H (2015) Microtopographic variation in soil respiration and its controlling factors vary with plant phenophases in a desert-shrub ecosystem. *Biogeosciences* 12:5705–5714. <https://doi.org/10.5194/bg-12-5705-2015>
- Wang B, Zha TS, Jia X, Gong JN, Bourque C, Feng W, Tian Y, Wu B, Zhang YQ, Peltola H (2017) Soil water regulates the control of photosynthesis on diel hysteresis between soil respiration and temperature in a desert shrubland. *Biogeosciences* 14:3899–3908. <https://doi.org/10.5194/bg-14-3899-2017>
- Yan L, Chen S, Huang J, Lin G (2011) Water regulated effects of photosynthetic substrate supply on soil respiration in a semi-arid steppe. *Glob Chang Biol* 17:1990–2001. <https://doi.org/10.1111/j.1365-2486.2010.02365.x>